Catalytic oxidation of diesel particulate matter by using silver and ceria supported on alumina as the oxidation catalyst

Sawatmongkhon, B.; Theinnoi, K.; Wongchang, T.; Haoharn, C.; Wongkhorsub, C.; Sukjit, E.; Tsolakis, A.

DOI:
10.1016/j.apcata.2019.01.020

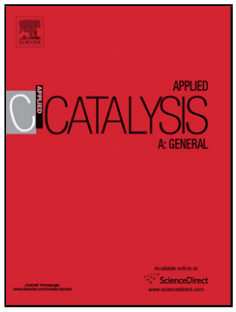

Title: Catalytic oxidation of diesel particulate matter by using silver and ceria supported on alumina as the oxidation catalyst

Authors: B. Sawatmongkhon, K. Theinnoi, T. Wongchang, C. Haoharn, C. Wongkhorsub, E. Sukjit, A. Tsolakis

PII: S0926-860X(19)30037-7
DOI: https://doi.org/10.1016/j.apcata.2019.01.020
Reference: APCATA 16960

To appear in: *Applied Catalysis A: General*

Received date: 2 November 2018
Revised date: 2 January 2019
Accepted date: 26 January 2019

Please cite this article as: Sawatmongkhon B, Theinnoi K, Wongchang T, Haoharn C, Wongkhorsub C, Sukjit E, Tsolakis A, Catalytic oxidation of diesel particulate matter by using silver and ceria supported on alumina as the oxidation catalyst, *Applied Catalysis A, General* (2019), https://doi.org/10.1016/j.apcata.2019.01.020

Catalytic oxidation of diesel particulate matter by using silver and ceria supported on alumina as the oxidative catalyst

B. Sawatmongkhon[a,b,*], K. Theinnoi[a,b], T. Wongchang[a,b], C. Haoharn[a,b], C. Wongkhorsub[a,b], E. Sukjit[c], A. Tsolakis[d]

[a] College of Industrial Technology, King Mongkut's University of Technology North Bangkok, 1518 Pracharat 1 Road, Wongsawang, Bangsue, Bangkok, 10800, Thailand.

[b] Research Centre for Combustion Technology and Alternative Energy (CTAE), Science and Technology Research Institute, King Mongkut's University of Technology North Bangkok, Thailand.

[c] School of Mechanical Engineering, Institute of Engineering, Suranaree University of Technology, Nakhon Ratchasima, 30000, Thailand.

[d] School of Mechanical Engineering, University of Birmingham, Birmingham B15 2TT, UK.

Graphical abstract

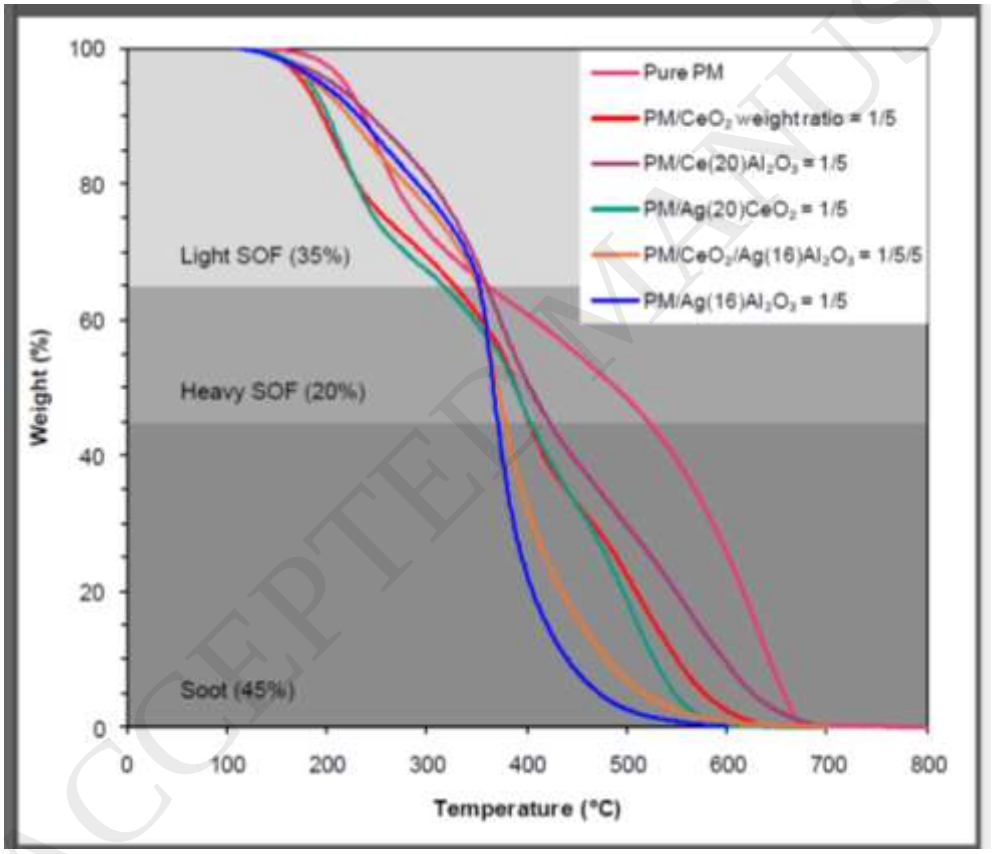

Highlights

- Silver enhances the combustion of heavy soluble organic fraction (SOF) and soot at high temperatures while ceria promotes the oxidation of light SOF at low temperatures.
- With 16 wt% silver supported on alumina, active temperatures are reduced from 400-700 °C (without catalyst) to 350-500 °C and more than 95% of diesel particulate matter (PM) is eliminated at 500 °C.

- The silver catalyst can be used by coating on a DPF's filter in order to control PM emitted from a diesel-engine passenger.

Abstract

To enable passive regeneration of a diesel particulate filter (DPF), this work seeks to study the potential of silver and ceria for the catalytic oxidation of diesel particulate matter (PM). Different contents of silver and ceria supported on alumina and silver loaded on ceria are synthesised by the incipient wetness impregnation method. The catalysts are characterised via XRD, SEM, and EDX. Catalytic PM oxidation performance for different PM/catalyst weight ratios and contact conditions is examined by using TGA. Removal of light soluble organic fraction (SOF) occurs between 110 and 350 °C through the vaporisation process. For the PM/catalyst weight ratio of 1/5, the silver compositions do not improve the depletion of light SOF but promote the combustion of both heavy SOF and soot, and the enhancement increases with silver content. For 16 wt% of silver supported on alumina, the PM/catalyst weight ratio of 1/20, and tight contact, oxidative activity is improved throughout the temperature window for light and heavy SOF and soot. The silver catalyst shows good stability for five runs. Active oxygen adspecies generated by ceria are different from those produced by silver. Enhanced performance for light SOF oxidation at a relatively low temperature is obtained using pure ceria. With the addition of alumina into ceria, light SOF removal ability of ceria is negatively affected. The positive effect on heavy SOF and soot reduction gained from the presence of silver is suppressed when ceria is mixed with silver.

Keywords: Diesel particulate matter, Silver catalyst, Ceria, Light SOF, Heavy SOF.

1. Introduction

Diesel particulate matter (PM), which consists of soluble organic fraction (SOF) and soot, is one of the regulated emissions emitted from diesel engines. To comply with stringent automotive emission standards, diesel particulate filters (DPF) have been effectively applied to control PM emissions. First, PM is entrapped by porous walls inside the DPF. Then, to avoid the back pressure created from the trapped PM, the DPF must be regenerated. In the regeneration process, oxidation of PM is carried out to make the filter re-usable. Without either a catalyst material coated on the filter or the assistance of a highly active oxidiser such as NO_2, PM is completely oxidised by oxygen only at the temperatures higher than 600 °C [1–3], which is much higher than the exhaust temperature of a light-duty diesel engine.

It is widely accepted that NO_2 is more active than O_2 for oxidation of PM [4–6]. Due to its high activity, a platinum based catalyst is generally applied to generate NO_2 from NO and O_2 [7–10]. Nevertheless, the main concern about platinum is its high cost. Currently, alternative materials, such as copper [11–13] and cobalt [14,15], have been employed to improve production of NO_2. However, the design of the modern diesel engine [16] and diesel fuel [17,18] tends to reduce NO_x formation, hindering the NO_2 assistance strategy.

In the absence of NO_2, active oxygen, such as peroxide (O_2^{2-}) and superoxide (O_2^-), plays a key role in the catalytic oxidation of carbon. Active oxygen was originally formulated from gas-phase oxygen with the assistance of a reducible metal [19]. Ceria-based catalyst is attractive for catalytic oxidation of PM due to its redox behaviour in which lattice oxygen acts as an active site

for the generation of active oxygen [20]. Due to its relatively low heat of oxygen chemisorption, ceria shows a high soot oxidation rate [21]. Ceria calcined at 800 °C (compared to 450 °C) has lower activation energy and a higher pre-exponential factor that lead to higher activity for soot oxidation [22,23]. Since the catalytic oxidation of PM is a solid-solid reaction, the number of contact points between the PM and the catalyst is crucially important. Therefore, several ceria-based catalyst morphologies have been studied. It was shown that a high specific surface area ceria catalyst synthesised in the form of three-dimensional stars has high soot-oxidation activity due to its high surface oxygen availability [24]. Doping ceria with transition metal was shown to have a positive effect on the formation of active oxygen on the catalytic site, which consequently enhanced the activity of catalytic soot oxidation [19,25].

The silver (Ag) supported catalyst has recently attracted increased attention because it is highly promising and affordable [26–30]. The catalyst promoted the formation of adsorbed active oxygen [31] including both peroxide and superoxide [32]. It was shown that the presence of Ag^+ on Ag nanoparticles gives rise to the high soot combustion activity by facilitating the initiation and migration of activated oxygen species [3,33]. With Ag (5%wt) loaded on CeO_2, the reaction rate of soot oxidation was increased by a factor of 10, and two reaction pathways for the promotion effect of Ag were proposed [34]. In the first reaction mechanism, Ag accelerated the formation of atomic oxygen from both the dissociative adsorption of gaseous O_2 and the migration of ceria bulk oxygen; the formed atomic oxygen then transferred onto the soot and gave rise to catalytic oxidation. In another scheme, first, O_2 adsorbed dissociatively on Ag, and then it spilled over onto the ceria to react with O^- and form highly active superoxide. Migration of active oxygen between Ag and support oxides (e.g., CeO_2 and MnO_x) was proposed as the critical feature for the high soot combustion rate [35,36]. Stability of silver catalysts under oxidative conditions is critical for PM oxidation. Although Ag_2O showed high activity, it was completely deactivated after the first catalytic run. Ag_2O did not act as a catalyst but did act as a strong oxidant. Atomic oxygen in Ag_2O chemically reacted with PM, and then Ag_2O was irreversibly transformed into Ag [27]. Later, the authors investigated the deactivation of Ag/SnO_2 for soot oxidation and found that self-regeneration was responsible for the catalyst stability [37]. Corro et al. [38] studied the PM oxidation stability of Ag/SiO_2 during six PM combustion cycles. They found that T_{max} (the temperature at which the maximum activity is obtained) during the first run was 350 °C, while, interestingly, during the subsequent cycles, the T_{max} decreased markedly from 350 to 230 °C. The authors proposed that during the first cycle, atomic oxygen in Ag_2O was strongly reduced by carbon to form metallic Ag^0, and during the subsequent cycles, metallic Ag^0 promoted the formation of highly active superoxide ions. Moreover, to confirm the reduction phenomena of Ag_2O during the first run of calcined Ag/SiO_2, the catalyst was first reduced by hydrogen, and then six cycles of catalytic PM oxidation were conducted. All six studies gave the similar T_{max} of 250 °C. In a recent work, it was concluded that the lack of changes in the electronic state of Ag during PM oxidation was the key factor for the catalyst stability [39].

In this work, different contents of silver (e.g., 2, 4, 8, and 16 wt%) and ceria (e.g., 5, 10, and 20 wt%) were supported on alumina and were applied as the PM oxidation catalysts. Catalytic activity was examined by thermogravimetric analysis (TGA). The effect of the contact area between the PM and the catalyst on the catalytic combustion potential was investigated by mixing the PM and catalyst at various weight ratios (e.g., 1/5, 1/10, 1/15, and 1/20). Silver catalyst stability was tested by carrying out five PM combustion cycles. To study the contact conditions, both tight and loose contacts were employed. To combine the positive aspects of

both silver and ceria, silver supported on the ceria catalyst with different silver contents (e.g., 5 and 20 wt%) was synthesised and used for PM catalytic oxidation.

2. Experimental

2.1. Material preparation

The silver supported on alumina catalyst was prepared via incipient wetness impregnation. Proper amounts of silver nitrate (Thomas Baker Chemicals, India) were dissolved in an appropriate quantity of distilled water to obtain metal loadings of 2, 4, 8, and 16 wt%. Then, the precursor solution was added dropwise to powdered γ-alumina (Ajax Finechem, Australia, BET of 142 m^2/g). The preparation of ceria supported on alumina was performed in the same manner with an appropriate amount of cerium(III) nitrate hexahydrate (Aldrich, 99% trace metals basis). To synthesise silver loaded on ceria, a calculated amount of aqueous silver nitrate was dropped on cerium(IV) oxide powder (Aldrich, 99.9% trace metals basis, particle size < 5 μm). Then, the solvent was removed by drying at 110 °C for 8 hrs in an oven. Then, the dry sample was calcined in static air at 600 °C with a heating rate of 10 °C/min for 2 hrs. Henceforth, the catalysts are denoted as X(Y)Z, where X represents the metal with Y wt% loading on Z support (e.g., $Ag(16)Al_2O_3$).

PM was directly taken from the exhaust gas of a traditional diesel engine. The engine was operated at a speed of 1000-2000 rpm and load of 25-75% of the maximum load. A stainless steel mesh was rolled at one round and placed inside the exhaust pipe (50 mm ID); then, the trapped PM was collected and dried in a furnace at 110 °C for 8 hrs. The dry PM was kept in an air tight container for subsequent experiments.

2.2. Catalyst characterisation

Crystal structures of the prepared catalysts were examined by X-ray diffraction (XRD). Diffractograms were recorded on a BRUKER D2 PHASER X-ray diffractometer using an X-ray source of Cu-Kα radiation operated at the accelerating voltage of 30 kV and current of 10 mA and equipped with a LYNXEYE XE detector. The diffraction intensity were collected using a step size of 0.02° and a scan speed of 1.2°/min in the range of $10° \leq 2\theta \leq 90°$. The diffraction peaks of crystalline phases were identified using the International Centre for Diffraction Data (ICDD) database. A ZEISS AURIGA field emission scanning electron microscope (FE-SEM) together with an Oxford Instruments energy-dispersive X-ray (EDX) spectrometer was used to obtain microscopic images of the catalysts and to characterise their elemental compositions. An aperture size of 30 μm was applied for the whole analysis. Accelerating voltages of 3 kV and 10 kV were used to obtain the images and elemental compositions, respectively.

2.3. Catalytic tests

Catalytic oxidation activity of PM was examined using the TGA method (PerkinElmer® Pyris 1). PM (10 mg) was physically mixed with the catalyst at the designed weight ratio for 5 min in a stainless steel mortar to obtain the tight contact mode or was shaken for 5 min in a glass tube for the loose contact conditions. Then, the mixture (≈10 mg) was sampled and placed in a ceramic crucible and heated from room temperature to 700 °C at a heating rate of 10 °C/min. Purified oxygen (99.999% purity) with a constant flow rate of 50 cm^3/min was used as the oxidiser. The sample weight was recorded continuously with the change in the temperature. The catalytic activity was assessed by using the following: T_{10}, defined as the onset temperature at which 10% of PM was removed; T_{55}, defined as the temperature at which soluble organic

fraction (SOF) contained in PM (55%) was completely consumed; T_{90}, defined as the temperature at which 90% of PM was depleted; and T_{max}, defined as the temperature at which the maximum rate of PM oxidation was observed.

3. Results and discussion

3.1. Properties of catalysts

Figure 1 shows the XRD profiles of the structures of the studied catalysts. The presence of the peaks (planes) at 38.2° (1 1 1), 44.4° (2 0 0), 64.5° (2 2 0), 77.3° (3 1 1), and 81.4° (2 2 2) [29,40] of Ag supported on both Al_2O_3 and CeO_2 indicates that after calcination at 600 °C, Ag is found in the form of metallic Ag. Other forms of Ag, such as AgO and Ag_2O, were not detected by XRD. According to Aneggi et al. [26], the large Ag_2O particles formed on Al_2O_3 and CeO_2 are thermally decomposed into metallic Ag during calcination by forming the metal state at the top of Ag_2O. At a relatively low content of Ag, such as $Ag(2)Al_2O_3$ and $Ag(4)Al_2O_3$, no Ag peaks were detectable indicating a good dispersion of Ag. The fluorite-like structure of CeO_2 presents the peaks (planes) at 28.5° (1 1 1), 33.1° (2 0 0), 47.5° (2 2 0), 56.3° (3 1 1), 59.1° (2 2 2), 69.3° (4 0 0), 76.6° (3 3 1), 79.1 (4 2 0), and 88.5 (4 2 2) [14,40].

The results obtained by SEM for different contents of Ag supported on Al_2O_3 are compared in Figure 2. Large Ag particles with the size of 1-2 μm are widely distributed on the Al_2O_3 surface for a relatively high Ag loading. Compared to $Ag(8)Al_2O_3$, $Ag(16)Al_2O_3$ shows a higher density of the large Ag particles. At the relatively low loading of Ag, the large Ag particles are absent, indicating that small Ag particles were dispersed into small pore of Al_2O_3. These results coincide with the results of the XRD measurements. As shown in Figure S1 (Supplementary Information) for $Ag(16)Al_2O_3$, O, Ag, and Al elements were identified by EDX. The Ag map confirms the excellent distribution of Ag.

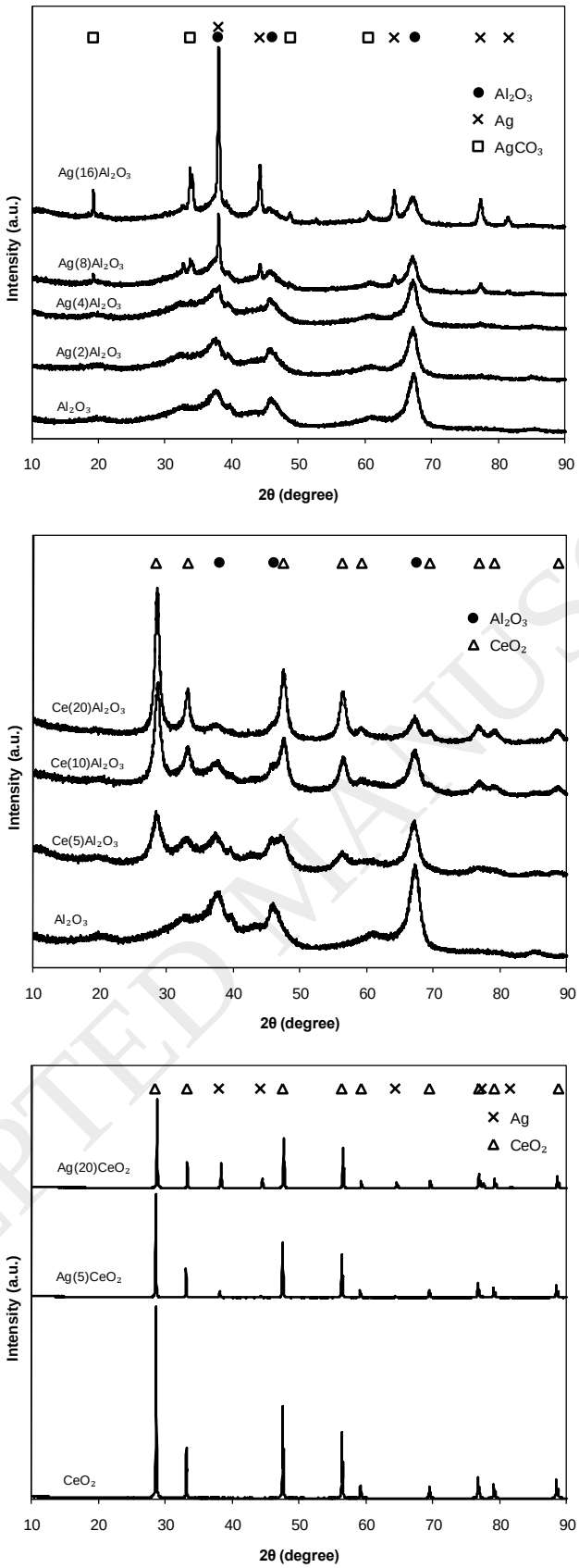

Figure 1. XRD profiles of $Ag(2)Al_2O_3$, $Ag(4)Al_2O_3$, $Ag(8)Al_2O_3$, $Ag(16)Al_2O_3$, $Ce(5)Al_2O_3$, $Ce(10)Al_2O_3$, $Ce(20)Al_2O_3$, $Ag(5)CeO_2$, and $Ag(20)CeO_2$.

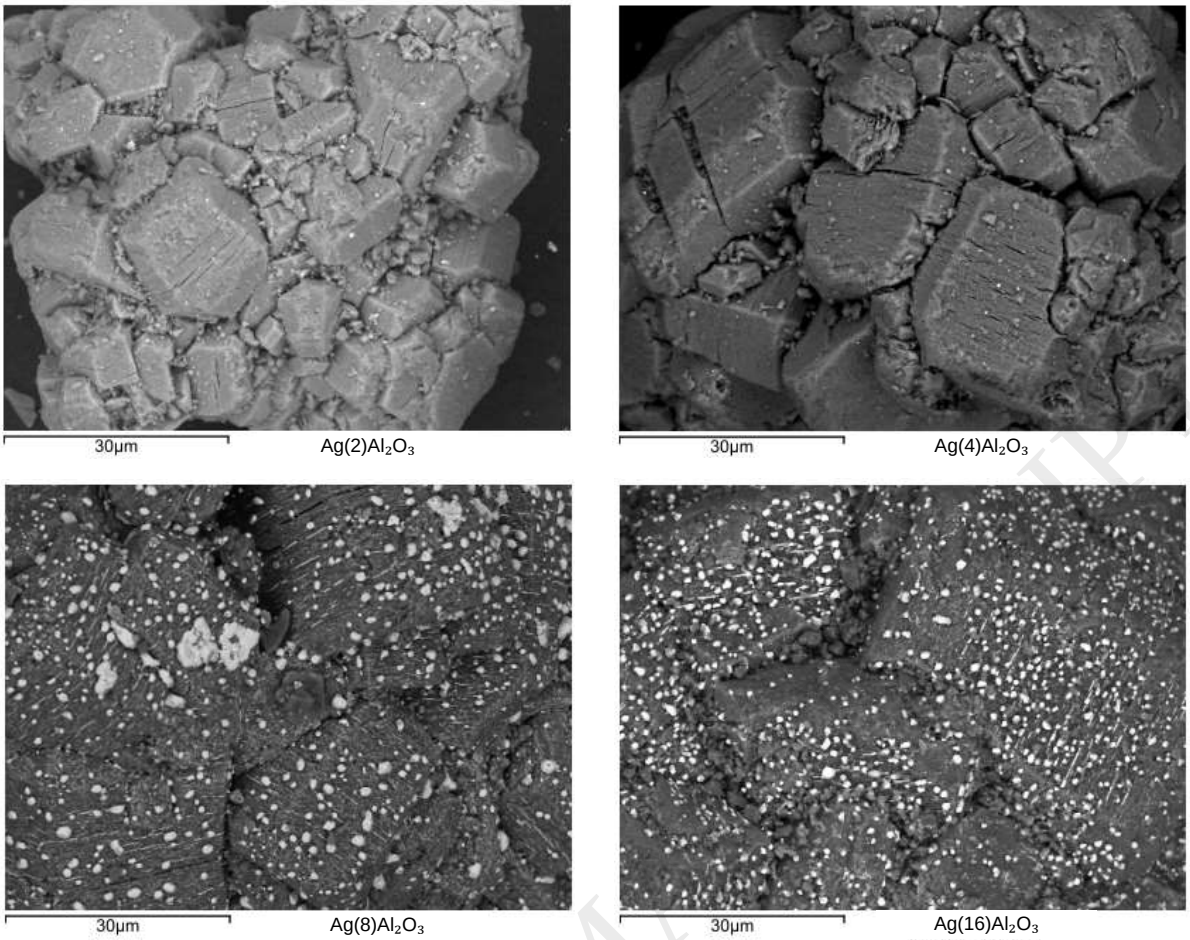

Figure 2. SEM images of $Ag(2)Al_2O_3$, $Ag(4)Al_2O_3$, $Ag(8)Al_2O_3$, and $Ag(16)Al_2O_3$.

3.2. Effect of silver on PM oxidation

PM composition in terms of SOF and soot was quantified by using the method of proximate analysis as presented in Figure S2 (Supplementary Information). Dry PM was heated from room temperature to 700 °C with a heating rate of 10 °C/min under N_2 and, then, the purge gas was switched to O_2 and held for 30 min. The contents of SOF and soot are 55 and 45%, respectively. SOF, which is the main component of PM, is usually ignored in the literature because it is assumed to be oxidised rapidly before the start of soot oxidation. Carbon black which consists of pure graphite is generally found as surrogate PM. Although the physical characteristics of model soot (graphite) and diesel soot are similar, the presence of SOF in PM results in a lower starting temperature and a higher rate of combustion than those of the surrogate soot [1,41,42].

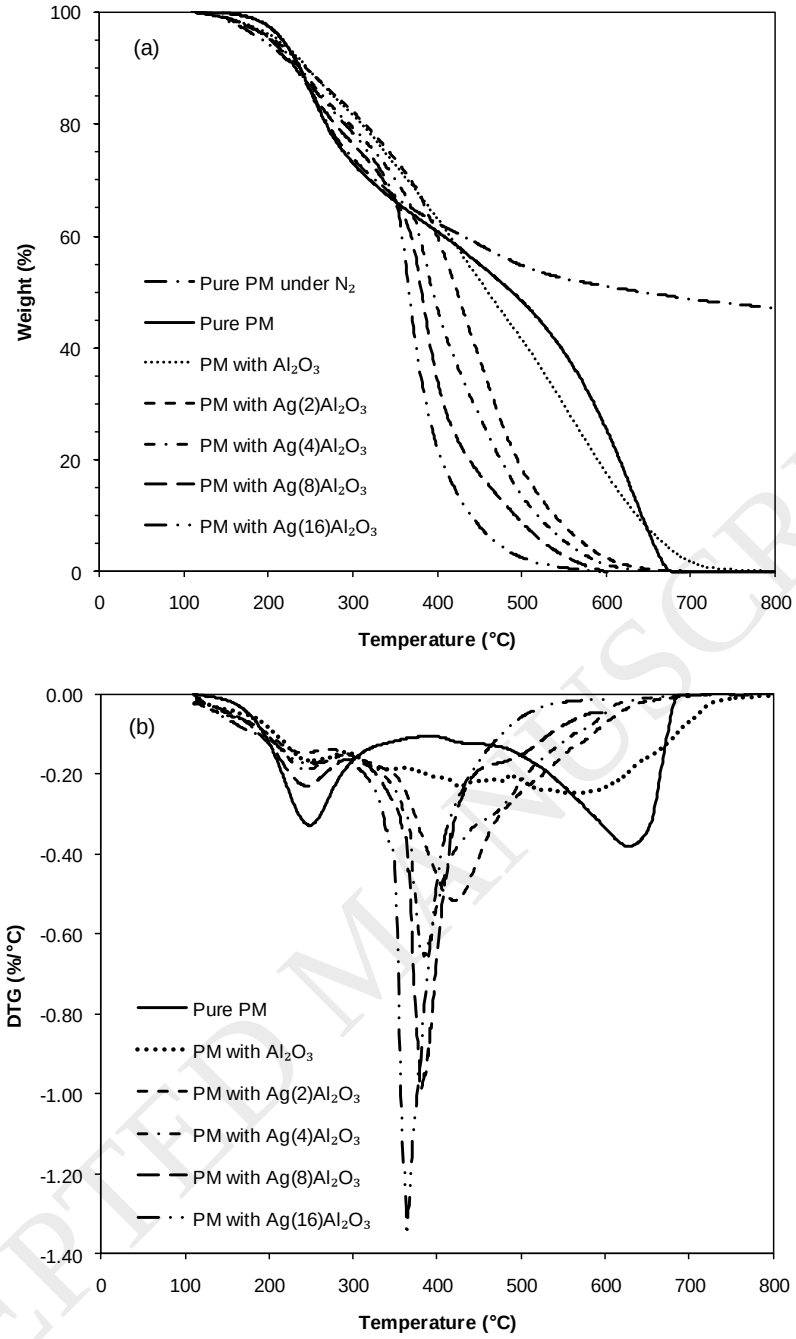

Figure 3. Thermogravimetric (a) and first derivative (b) profiles of PM oxidation; tight contact mode; PM/catalyst weight ratio of 1/5.

Figure 3 presents the thermogravimetric (TG) profile and its first derivative (DTG) for PM oxidation under the tight contact mode and the PM/catalyst weight ratio of 1/5. Two obvious DTG peaks of each sample observed in Figure 3b at the relatively low and high temperatures confirm the existence of SOF and soot. Without the addition of a catalyst, the two peaks at 253 and 637 °C of pure PM indicate that SOF and soot are oxidised at the maximum rate at these temperatures, respectively; and the maximum oxidation rate of soot is slightly greater than that of SOF. The presence of two DTG peaks indicates the complexity of the PM oxidation mechanism that contains at least two rate-determining steps [43]. As shown in Figure 3a, the weight loss of PM mixing with alumina is monotonically reduced, illustrating the inert

behaviour of alumina. Interestingly, as shown in Figure 3a, the weight loss profiles of pure PM under both N_2 and O_2, coincide in the temperature range of 110-350 °C. This indicates that the depletion of some SOF occurs without the assistance of O_2. SOF depletion may be due to vaporisation and/or thermal cracking. However, at the temperatures below 350 °C, it is difficult for SOF to thermally decompose. Therefore, it can be concluded that the largest fraction of SOF (35%) are removed from PM by the vaporisation process at the temperatures below 350 °C. The SOF that is active in this temperature range consists mainly of polyaromatic hydrocarbons (PAHs) with three and four rings [42]. Henceforth, these PAHs are referred to as light SOF. Diehl et al. [44] also found that the vaporisation of highly volatile hydrocarbons was the main pathway of SOF migration. As the silver content increases, the intensity of the first DTG peak at a relatively low temperature decreases while the second DTG peak becomes larger. The shift of the second DTG peak to lower temperatures describes the promotion effect of silver on PM oxidation. This implies that the silver catalyst changes the rate-limiting step of the PM combustion mechanism. However, while the position of the first DTG peak remains unchanged, its intensity decreases with increasing silver fraction. This suggests that the normal vaporisation of light SOF is retarded by added substances. At temperatures higher than 350 °C, in the absence of a catalyst, PM starts to be oxidised directly with gas-phase oxygen, as can be easily seen from the divergence of the weight loss profiles of pure PM under N_2 and O_2. In the presence of silver loaded on alumina, PM oxidation is strongly promoted. The direct activation of PM and gas-phase oxygen is replaced by a highly active pathway in which according to the literature [26], silver in both metal and metal oxide forms facilitates the activation of gas-phase oxygen into highly active oxygen adspecies. Removal of PM depends directly on silver composition. At a relatively high silver content, the high density of the large silver particles formed on alumina, as shown in Figure 2, lead to more points of contact between PM and silver; accordingly, higher PM oxidation activity is obtained. For $Ag(16)Al_2O_3$, the active temperature is decreased from 400-700 °C (without the catalyst) to 350-500 °C and more than 95% of PM is eliminated at 500 °C. This new temperature window is suitable for the exhaust-gas temperature of a passenger car diesel engine, demonstrating the potential of the silver catalyst in PM control technology.

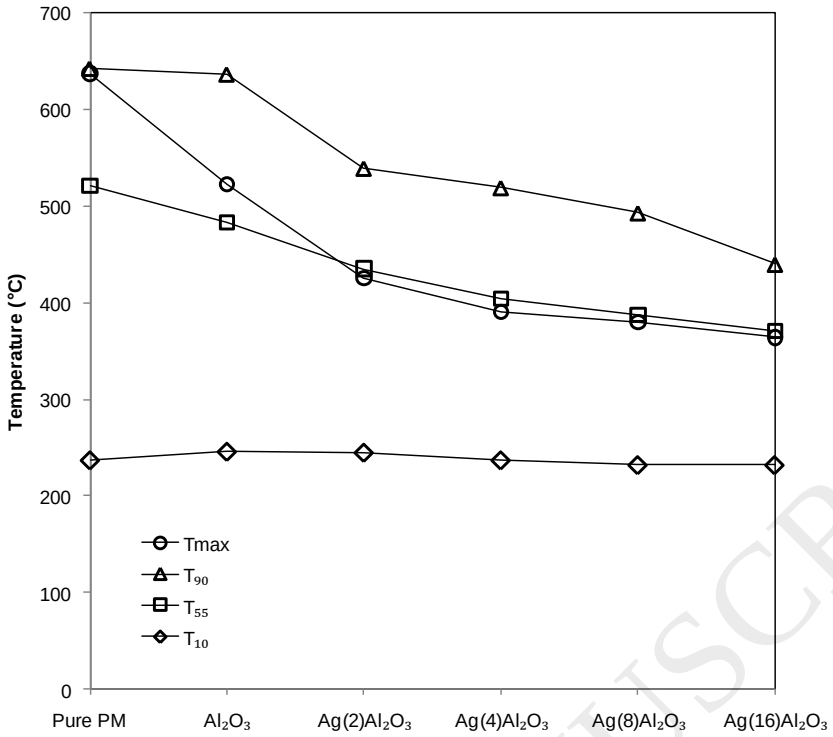

Figure 4. PM oxidation performance of catalysts with different silver contents supported on alumina in the tight contact mode and with the PM/catalyst weight ratio of 1/5.

The PM oxidation performance in terms of T_{10}, T_{55}, T_{90}, and T_{max} of the catalysts with different silver loadings is presented in Figure 4. The similarity in the values of the onset temperature T_{10} of all of the samples reveals that the initiation of the PM oxidation process is not accelerated by the catalyst. As already stated, the initial stage of diesel-PM oxidation occurs through the vaporisation of light SOF. T_{55} is considerably reduced in the presence of the silver catalyst. Silver shows a remarkable positive effect by decreasing T_{55} from 521 °C for pure PM to 371 °C in the presence of $Ag(16)Al_2O_3$. The reduction of T_{55} suggests that catalytic oxidation of all parts of SOF is completed at an early stage by the oxidiser which is not the gas-phase oxygen but rather the active oxygen that is formed from gas-phase oxygen and facilitated by silver. As explained above, the removal of light SOF is not accelerated by silver. Therefore, the decrease of T_{55} is caused by the catalytic oxidation of remaining SOF which is henceforth referred to as heavy SOF. Therefore, not only soot but also heavy SOF is catalytically oxidised by the active oxygen created on silver sites. T_{90} drops from 650 °C for the oxidation of pure PM to 440 °C in the presence of $Ag(16)Al_2O_3$. T_{90} is critically important because it is used to identify the temperature required to oxidise PM almost completely. For the $Ag(16)Al_2O_3$ catalyst, the exhaust temperature of 440 °C is necessary to effectively regenerate a DPF. T_{max} also follows the same trend as T_{55} and T_{90} and decreases with increasing silver content. Interestingly, T_{max} obtained from all of the catalysts, regardless of silver content, is slightly less than T_{55}, confirming the promotional effect of silver on both heavy SOF and soot combustion. Normally, the reaction rate of solid material is directly dependent on the availability of the solid [43]. In this situation, both heavy SOF and all of the soot contained in PM are still available at the beginning of catalytic oxidation; thus, the maximum rate is obtained.

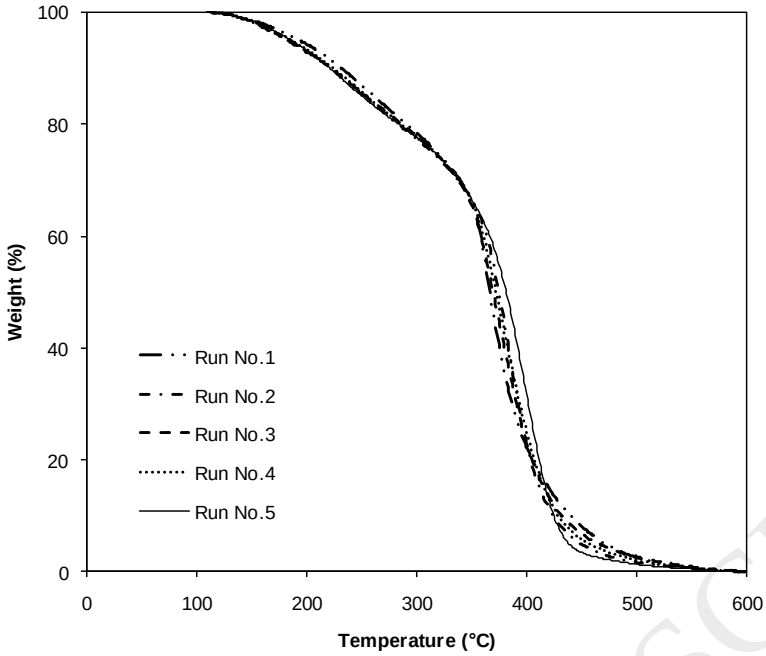

Figure 5. Weight loss profile illustrating the stability of the $Ag(16)Al_2O_3$ catalyst on PM oxidation in the tight contact mode for the PM/catalyst weight ratio of 1/5.

To verify the reproducibility of data obtained, three runs of fresh $Ag(16)Al_2O_3$ which was tightly mixed with PM at the PM/catalyst weight ratio of 1/5 was conducted. The weight loss profiles show excellent reproducibility. The $Ag(16)Al_2O_3$ catalyst was further investigated in terms of PM oxidation stability since it shows the best performance. To examine the catalyst stability, the PM oxidation test was performed five times using the same catalyst. The weight loss profiles shown in Figure 5 indicate the excellent stability of the catalyst. As mentioned in the Introduction, the catalytic activity of Ag_2O suddenly vanished after the first run; therefore, the active site of $Ag(16)Al_2O_3$ is not Ag_2O. Based on this result and the results of the XRD measurements, it can be concluded that metallic Ag is the active component of the silver catalyst.

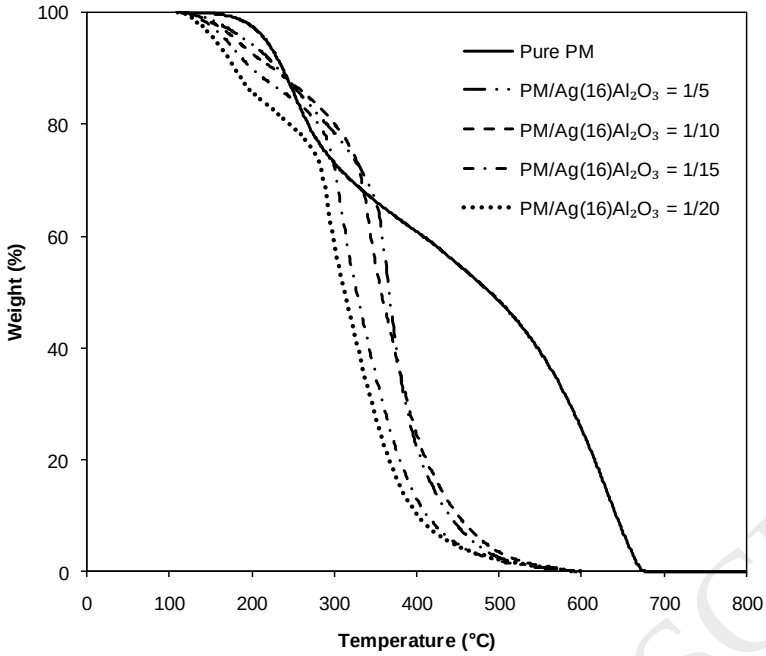

Figure 6. Effect of the PM/catalyst weight ratio on PM oxidation using the $Ag(16)Al_2O_3$ catalyst in the tight contact mode.

The impact of contact points between the PM and catalyst on the catalytic PM oxidation was investigated by conducting activity tests with different PM/catalyst weight ratios. The mixtures of PM and catalyst were prepared in the tight contact mode with the PM/catalyst weight ratios of 1/5, 1/10, 1/15, and 1/20. Figure 6 shows that the number of contact points plays a crucial role in PM combustion [34]. The oxidation activity increases substantially with the weight ratio, especially for the change from 1/10 to 1/15. This may indicate that the weight ratio of 1/15 is appropriate for the catalysed PM oxidation. For the removal of light SOF, although the silver catalyst shows less activity than pure PM, its performance improves as the weight ratio increases. This result reveals that the catalytic oxidation of light SOF promoted by silver occurs concurrently with the vaporisation of light SOF, but its rate is lower than the rate of vaporisation. It is observed that as the weight ratio increases to 1/20, the light SOF oxidation performance of the silver catalyst is better than that of pure PM. This is the only PM/catalyst weight ratio for which the reduction of light SOF is better than the reduction of pure PM. As shown above, removal of light SOF occurs mainly via the vaporisation process which means that the light SOF is not chemically transformed into benign gaseous substances but rather is vaporised into the vapour state. The light SOF can then condense again at a low temperature. Therefore, it is important to permanently eliminate the light SOF through catalytic oxidation. A mechanical mixture of Pt/SiC into soot oxidation catalyst was used to address the SOF [42]. For the PM/catalyst weight ratio of 1/20, the depletion of light SOF no longer follows the vaporisation pathway. The route of light SOF conversion should be investigated in future work.

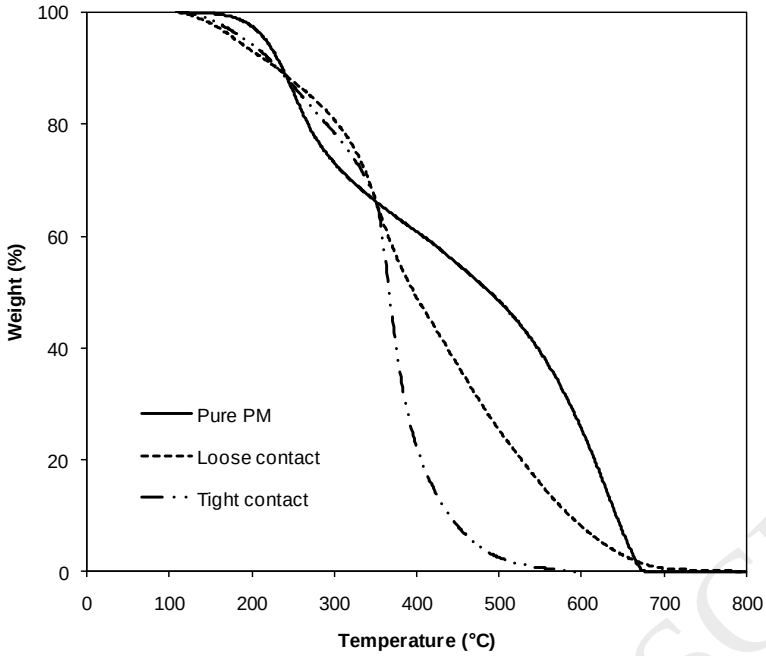

Figure 7. Influence of the contact mode on the PM oxidation activity for the Ag(16)Al_2O_3 catalyst with the PM/catalyst weight ratio of 1/5.

Figure 7 presents the effect of PM-Ag(16)Al_2O_3 contact regime on catalytic PM oxidation. Interestingly, at the temperatures lower than 370 °C, the similar weight loss profiles of the PM-catalyst mixtures in both tight and loose conditions indicate that the contact conditions do not affect the vaporisation of light SOF. At the temperatures higher than 370 °C, the catalyst shows considerable promotion of PM combustion. The remaining heavy SOF content of 20% (55% of PM is SOF, with 35% of PM comprised of light SOF that is destroyed at the temperatures below 370 °C) is catalytically oxidised by the catalyst. The weight loss of both heavy SOF and soot is significantly improved in the tight contact conditions. The tight mode provides close contact between the PM and the catalyst. Therefore, the active oxygen formed on silver sites can migrate onto the PM particles with a relatively short distance and, then catalytically oxidise the remaining PM. In the loose contact conditions, the relatively long length that must be travelled by the active oxygen results in low oxidation rates of both heavy SOF and soot.

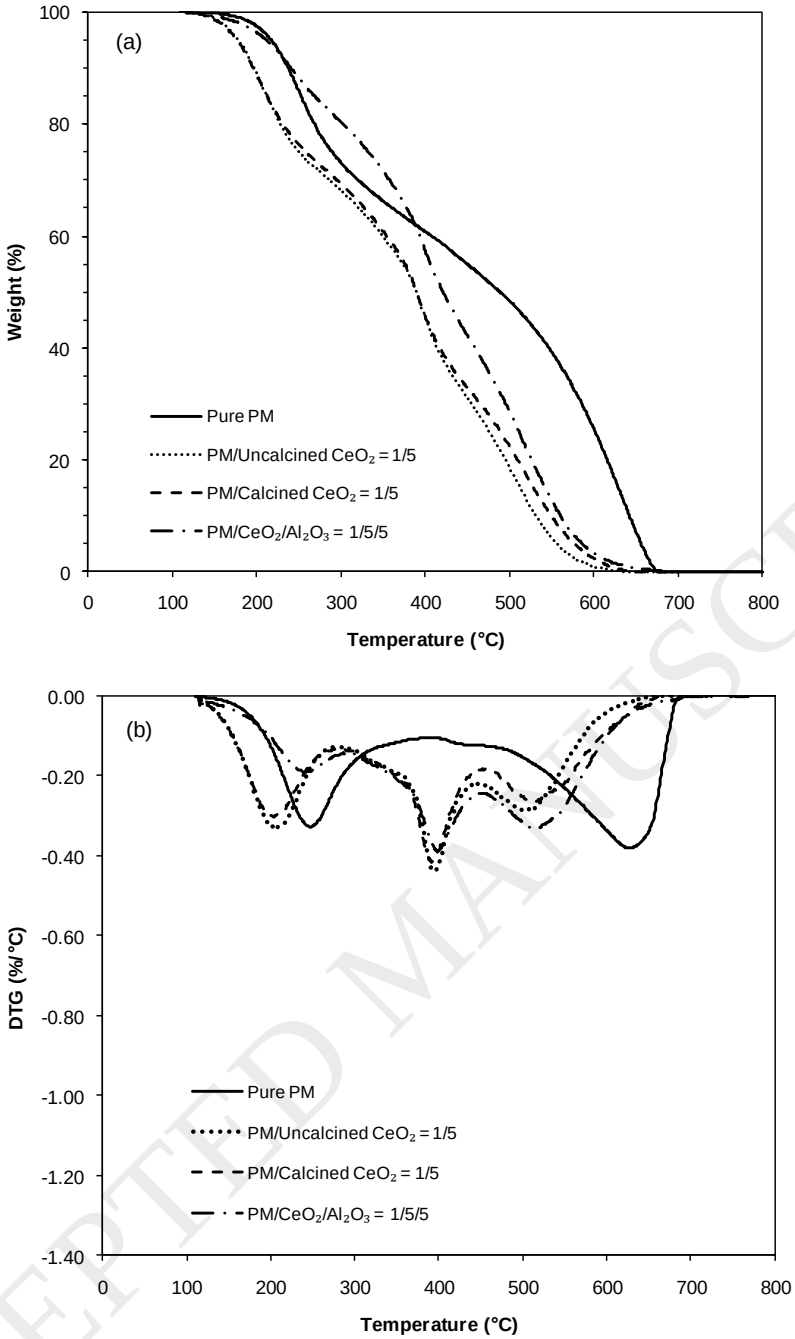

Figure 8. Effect of ceria on PM oxidation: thermogravimetric (a) and first derivative (b) profiles for the tight contact mode.

3.3. Effect of ceria on PM oxidation

The effect of ceria on PM oxidation is displayed in Figure 8. In this experiment, PM was physically and tightly mixed with either uncalcined or calcined ceria at the PM/ceria weight ratio of 1/5. The calcination was carried out in static air at 600 °C with a heating rate of 10 °C/min for 2 hrs. As shown in Figure 8a, similar PM combustion reactivities were obtained for both uncalcined and calcined ceria, and their performances are better than for pure PM throughout the temperature window. Interestingly, the removal of light SOF for which the silver catalysts do not show a promotional effect is significantly improved by both ceria treatments. As

observed in Figure 8b, both ceria treatments shift the first DTG peak from 250 to 200 °C, indicating that ceria changes the rate-determining step of light SOF depletion from the vaporisation process to the catalytic oxidation of light SOF. Moreover, three DTG peaks are clearly observed. The second DTG peak at 400 °C illustrates the enhancement of heavy SOF combustion. The third DTG peak indicates that the rate of soot elimination reaches the maximum value at 520 °C; however, the rate is relatively low. Fascinatingly, when PM, ceria, and alumina are physically mixed together with the weight ratio of 1/5/5, there is no positive effect of ceria on light SOF oxidation. The first DTG peak of the mixture returns to the temperature similar to that of pure PM (250 °C). This shows that the catalytic oxidation of light SOF assisted by ceria is replaced by the vaporisation. In summary, manually added alumina destroys the ability of ceria to chemically remove the light SOF.

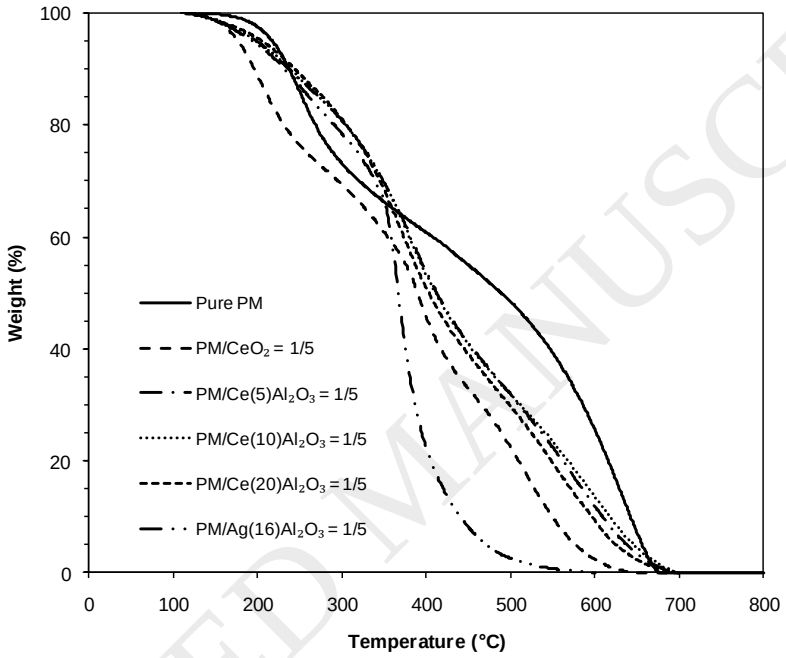

Figure 9. Impact of ceria content loaded on alumina on PM oxidation for tight contact and the PM/catalyst weight ratio of 1/5.

To verify the negative effect of alumina on ceria as presented in Figure 8, different ceria contents are impregnated on alumina and their impact on PM oxidation is shown in Figure 9. The obtained results confirm that the presence of alumina harms the ability of the ceria to perform the catalytic oxidation of light SOF at relatively low temperatures. As the ceria fraction increases by a factor of four (from 5 to 20 wt%), there is a small effect on the PM oxidation activity. Compared to the mechanical mixture between PM and pure ceria, ceria supported on alumina gives considerably low PM reduction performance.

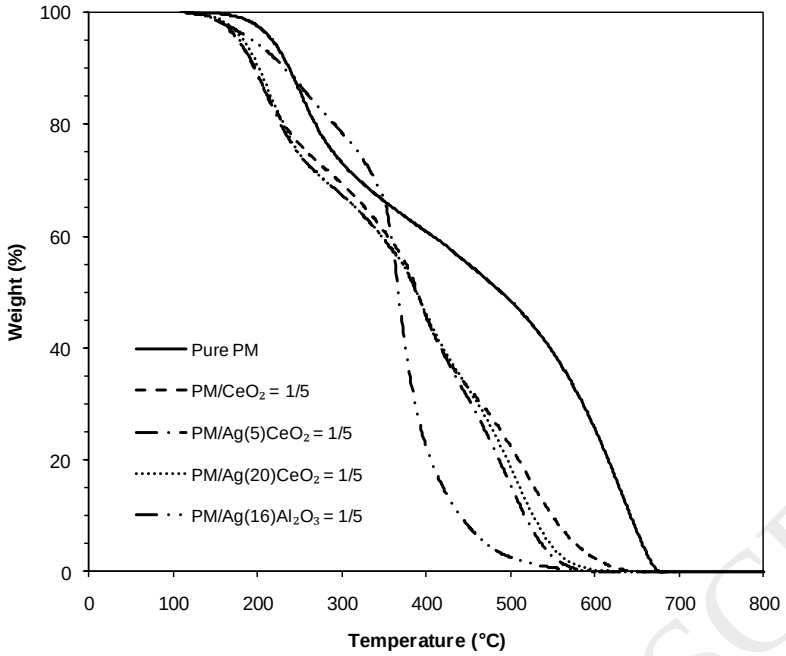

Figure 10. Effect of silver supported on ceria on PM oxidation for tight contact and the PM/catalyst weight ratio of 1/5.

As discussed above, ceria (without added alumina) promotes the oxidation of light SOF at relatively low temperatures and silver improves the reduction activity of heavy SOF and soot at relatively high temperatures. Accordingly, the advantages of both substances are combined by synthesising silver supported on ceria. The performance of the obtained catalyst is depicted in Figure 10. Regardless of the presence of silver, ceria shows improvement of light SOF elimination, indicating that the activation of the oxidiser used to chemically react with light SOF was carried out on ceria sites. However, at relatively high temperatures, the expected enhancement of heavy SOF and soot depletion was not obtained. Moderate improvement was gained from the addition of silver to ceria. Lee et al. [29] also found a moderate improvement for the Ag/CeO_2 catalyst. It is likely that the presence of ceria prevents the creation of highly active adspecies formed on the silver sites and used to oxidise heavy SOF and soot. This indicates that activation of gas-phase oxygen occurs preferentially on the ceria sites. Moreover, a factor of four increase in the silver content (from 5 to 20 wt%) has a slight effect on the PM reduction activity. This verifies that the major pathway yielding active oxygen occurs on the ceria rather than on the silver sites. In the absence of ceria, $Ag(16)Al_2O_3$ shows high activity for the oxidation of heavy SOF and soot. These results suggest that the active oxygen generated by ceria is different from that generated by silver; its formation rate on the ceria sites is faster than that of the active oxygen formed on the silver sites, and it is highly active for light SOF and has low activity for heavy SOF and soot.

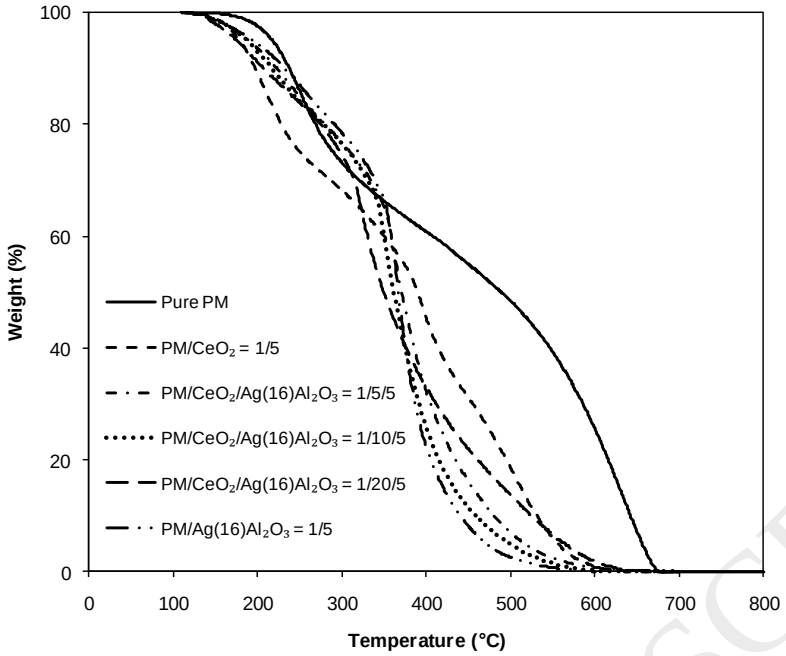

Figure 11. PM oxidation activity at different PM/CeO_2/Ag(16)Al_2O_3 weight ratios in tight contact.

PM oxidation performance for a physical combination of pure ceria with silver supported on the alumina catalyst is demonstrated in Figure 11. To improve the reduction of all of the three components of PM, pure ceria and Ag(16)Al_2O_3 were ground together with PM (tight contact) at different weight ratios. In the presence of silver catalyst, the predominant feature of pure ceria for oxidation of light SOF at relatively low temperatures deteriorated dramatically; this is similar to the results presented in Figure 8 and Figure 9. Thus, the presence of alumina leads to the loss of the ceria's capability to form active surface species used to oxidise light SOF. Fortunately, the positive effect of the silver catalyst on the combustion of heavy SOF and soot is still present. The inert behaviour of alumina is an important characteristic in its role as the silver support. Unlike the doping of silver on ceria, the mechanical mixture of the silver catalyst with ceria has a slight effect on the performance of the silver catalyst. For an increase in the weight ratio of PM/CeO_2/Ag(16)Al_2O_3 from 1/5/5 to 1/10/5, ceria slightly enhances light SOF reduction while the positive effect of the silver catalyst on the heavy SOF and soot oxidation is obvious. Interestingly, an increase in the ceria fraction from the weight ratio of 1/10/5 to that of 1/20/5 leads to an improvement in the combustion of both light and heavy SOF. However, the soot oxidation performance is considerably decreased. These phenomena confirm that two different types of active oxygen are separately formed from the gas-phase oxygen and are individually adsorbed on the ceria and silver sites.

4. Conclusion

Different compositions of silver and ceria catalysts were synthesised by incipient wetness impregnation. The performance for catalytic oxidation of diesel PM was examined by using the thermogravimetric approach. The diesel PM was composed of light SOF, heavy SOF, and soot with the fractions of 35, 20, and 45%, respectively. Silver supported on alumina plays an important role in increasing the oxidation rate of heavy SOF and soot at relatively high temperatures but has only a slight effect on the depletion of light SOF. Its catalytic ability increases with both increasing metallic silver fraction and increasing PM/catalyst weight ratio.

The silver catalyst shows good stability with five oxidation runs. Ceria shows high performance of light SOF removal at relatively low temperatures, but its catalytic ability is significantly reduced in the presence of alumina. Its capability to oxidise heavy SOF and soot is considerably lower than that of silver. Two different types of active oxygen are independently formed on ceria and silver sites. The former is highly active for light SOF, while the latter is responsible for the oxidation of heavy SOF and soot. The impregnation of ceria into silver reduces the ability of the silver to generate its active oxygen, resulting in low activity for the oxidation of heavy SOF and soot. Nevertheless, the physical combination of the silver catalyst with ceria has only a slight effect on the catalytic ability of the silver catalyst.

References

[1] A. Bueno-López, Appl. Catal. B Environ. 146 (2014) 1–11.

[2] R. Matarrese, S. Morandi, L. Castoldi, P. Villa, L. Lietti, Appl. Catal. B Environ. 201 (2017) 318–330.

[3] X. Deng, M. Li, J. Zhang, X. Hu, J. Zheng, N. Zhang, B.H. Chen, Chem. Eng. J. 313 (2017) 544–555.

[4] H. Muckenhuber, H. Grothe, Carbon N. Y. 44 (2006) 546–559.

[5] N. Zouaoui, M. Issa, D. Kehrli, M. Jeguirim, Catal. Today 189 (2012) 65–69.

[6] R. Matarrese, L. Castoldi, L. Lietti, Chem. Eng. Sci. 173 (2017) 560–569.

[7] A. Setiabudi, J. Chen, G. Mul, M. Makkee, J.A. Moulijn, Appl. Catal. B Environ. 51 (2004) 9–19.

[8] S. Liu, X. Wu, D. Weng, M. Li, J. Fan, Appl. Catal. B Environ. 138–139 (2013) 199–211.

[9] M. Jeguirim, V. Tschamber, P. Ehrburger, Appl. Catal. B Environ. 76 (2007) 235–240.

[10] V.R. Pérez, A. Bueno-López, Chem. Eng. J. 279 (2015) 79–85.

[11] T. Andana, M. Piumetti, S. Bensaid, L. Veyre, C. Thieuleux, N. Russo, D. Fino, E.A. Quadrelli, R. Pirone, Appl. Catal. B Environ. 216 (2017) 41–58.

[12] A. Bueno-López, D. Lozano-Castelló, A.J. McCue, J.A. Anderson, Appl. Catal. B Environ. 198 (2016) 266–275.

[13] J. Giménez-Mañogil, A. Bueno-López, A. García-García, Appl. Catal. B Environ. 152–153 (2014) 99–107.

[14] J. Xu, G. Lu, Y. Guo, Y. Guo, X.-Q. Gong, Appl. Catal. A Gen. 535 (2017) 1–8.

[15] M.Á. Stegmayer, V.G. Milt, N. Navascues, E. Gamez, S. Irusta, E.E. Miró, Mol. Catal. (2018).

[16] S.S. Gill, G.S. Chatha, A. Tsolakis, Int. J. Hydrogen Energy 36 (2011) 10089–10099.

[17] K. Theinnoi, A.P.E. York, A. Tsolakis, S. Chuepeng, R.F. Cracknell, R.H. Clark, Int. J. Veh. Des. 50 (2009) 196–212.

[18] K. Theinnoi, A. Tsolakis, S. Sitshebo, R.F. Cracknell, R.H. Clark, Chem. Eng. J. 158 (2010) 468–473.

[19] D. Mukherjee, B.G. Rao, B.M. Reddy, Appl. Catal. B Environ. 197 (2016) 105–115.

[20] A. Bueno-López, K. Krishna, M. Makkee, J.A. Moulijn, J. Catal. 230 (2005) 237–248.

[21] J.M. Christensen, J.-D. Grunwaldt, A.D. Jensen, Appl. Catal. B Environ. 188 (2016) 235–244.

[22] M.S. Gross, M.A. Ulla, C.A. Querini, J. Mol. Catal. A Chem. 352 (2012) 86–94.

[23] M.S. Gross, B.S. Sánchez, C.A. Querini, Chem. Eng. J. 168 (2011) 413–419.

[24] P. Miceli, S. Bensaid, N. Russo, D. Fino, Chem. Eng. J. 278 (2015) 190–198.

[25] X. Lin, S. Li, H. He, Z. Wu, J. Wu, L. Chen, D. Ye, M. Fu, Appl. Catal. B Environ. 223 (2018) 91–102.

[26] E. Aneggi, J. Llorca, C. de Leitenburg, G. Dolcetti, A. Trovarelli, Appl. Catal. B Environ. 91 (2009) 489–498.

[27] K. Shimizu, H. Kawachi, A. Satsuma, Appl. Catal. B Environ. 96 (2010) 169–175.

[28] K. Shimizu, H. Kawachi, S. Komai, K. Yoshida, Y. Sasaki, A. Satsuma, Catal. Today 175 (2011) 93–99.

[29] C. Lee, J.-I. Park, Y.-G. Shul, H. Einaga, Y. Teraoka, Appl. Catal. B Environ. 174–175 (2015) 185–192.

[30] C. Lee, Y.-G. Shul, H. Einaga, Catal. Today 281 (2017) 460–466.

[31] L. Nossova, G. Caravaggio, M. Couillard, S. Ntais, Appl. Catal. B Environ. 225 (2018) 538–549.

[32] Y. Zhao, Z. Wen, Y. Huang, X. Duan, Y. Cao, L. Ye, L. Jiang, Y. Yuan, Catal. Commun. 111 (2018) 26–30.

[33] M. Haneda, A. Towata, Catal. Today 242 (2015) 351–356.

[34] S. Liu, X. Wu, W. Liu, W. Chen, R. Ran, M. Li, D. Weng, J. Catal. 337 (2016) 188–198.

[35] K. Yamazaki, T. Kayama, F. Dong, H. Shinjoh, J. Catal. 282 (2011) 289–298.

[36] N. Guilhaume, B. Bassou, G. Bergeret, D. Bianchi, F. Bosselet, A. Desmartin-Chomel, B. Jouguet, C. Mirodatos, Appl. Catal. B Environ. 119–120 (2012) 287–296.

[37] K. Shimizu, M. Katagiri, S. Satokawa, A. Satsuma, Appl. Catal. B Environ. 108–109 (2011) 39–46.

[38] G. Corro, U. Pal, E. Ayala, E. Vidal, Catal. Today 212 (2013) 63–69.

[39] G. Corro, E. Vidal, S. Cebada, U. Pal, F. Bañuelos, D. Vargas, E. Guilleminot, Appl. Catal. B Environ. 216 (2017) 1–10.

[40] L. Yu, R. Peng, L. Chen, M. Fu, J. Wu, D. Ye, Chem. Eng. J. 334 (2018) 2480–2487.

[41] I. Atribak, A. Bueno-López, A. García-García, Combust. Flame 157 (2010) 2086–2094.

[42] R. Ramdas, E. Nowicka, R. Jenkins, D. Sellick, C. Davies, S. Golunski, Appl. Catal. B Environ. 176–177 (2015) 436–443.

[43] S. Vyazovkin, A.K. Burnham, J.M. Criado, L. a. Pérez-Maqueda, C. Popescu, N. Sbirrazzuoli, Thermochim. Acta 520 (2011) 1–19.

[44] F. Diehl, J. Barbier, D. Duprez, I. Guibard, G. Mabilon, Appl. Catal. A Gen. 504 (2015) 37–43.